

Accurate Nodes Localization in Anisotropic Wireless Sensor Networks

Ahmad El Assaf*, Slim Zaidi*, Sofène Affes*[†], and Nahi Kandil*[†]

*INRS-EMT, Université du Québec, Montreal, QC, H5A 1K6, Canada, Email: {elassaf,zaidi,affes}@emt.inrs.ca

[†]LRTCS, University of Quebec in Abitibi-Témiscaming, Rouyn-Noranda, QC, J9X 5E4, Canada, Email: nahi.kandil@uqat.ca

Abstract—An accurate localization algorithm tailored for anisotropic wireless sensors networks (WSNs) is proposed in this paper. Using the proposed algorithm, each regular or position-unaware node estimates its distances only to reliable anchors or position-aware nodes. The latter are properly chosen following a new reliable anchor selection strategy that ensures an accurate distance estimation making thereby our localization algorithm more precise. Simulations show that our algorithm, consistently outperforms the best representative localization algorithms currently available in the literature in terms of accuracy, even with the presence of non-uniform node distribution or radiation irregularities.

Index Terms—Anisotropic wireless sensor networks, localization algorithms, range-free, anchor selection.

I. INTRODUCTION

Due to their reliability, low cost, and ease of deployment, wireless sensor networks (WSNs) are emerging as a key tool for many applications such as environment monitoring, disaster relief, and target tracking [1]. A WSN is a set of small and low-cost sensor nodes with limited communication capabilities. The latter are often deployed in a random fashion to collect some physical phenomena from the surrounding environments such as temperature, light, pressure, etc. [2]. Due to their limited transmission ranges, the sensor nodes are often unable to directly communicate with a remote access point (AP). For this reason, they recur to multi-hop communication through several intermediate nodes that successively forward their gathered data to the AP. However, the sensing data are very often meaningless if the location from where they have been measured is unknown; which makes their localization a fundamental and essential issue in WSNs. So far, many localization algorithms have been proposed in the literature and mainly fall into two categories: range-based and range-free.

To properly localize the regular or position-unaware nodes, range-based algorithms exploit the measurements of the received signal characteristics such as the time of arrival (TOA), the angle of arrival (AOA), or the received signal strength (RSS) [3]-[5]. These signals are, in fact, transmitted by nodes having prior knowledge of their positions, called anchors (or landmarks). Although the range-based algorithms stand to be very accurate, they are unsuitable for WSNs. Indeed, these algorithms require high power to ensure communication between anchors and regular nodes which are small battery-powered units. Furthermore, additional hardware is usually required at both anchors and regular nodes, thereby increasing the overall cost of the network. Moreover, the performance of these algorithms can be severely

affected by noise, interference, and/or fading. Unlike range-based algorithms, range-free algorithms, which rely on the network connectivity to estimate the regular node positions, are more power-efficient and do not require any additional hardware and, hence, are suitable for WSNs [6]-[15]. Due to these practical merits, range-free localization algorithms have garnered the attention of the research community. Unfortunately, in anisotropic environments where obstacles and/or holes may exist, range-free algorithms do not provide sufficient accuracy due to large errors occurring when mapping the hops into distance units. Indeed, in such environments, it is very likely that the shortest path between an anchor and a regular node is curved, thereby resulting in overestimation of the distance between these two nodes. The more obstacles and/or holes there are, the larger are distance estimation errors and, consequently, less accurate is localization.

In this paper, we propose a novel range-free localization algorithm tailored for anisotropic WSNs. Using the proposed algorithm, each regular node estimates its distances only to reliable anchors. The latter are properly chosen following a new reliable anchor selection strategy that ensures an accurate distance estimation thereby making our localization algorithm more precise. New average hop sizes' expressions are also developed in this paper for both 2-D and 3-D scenarios. Simulations show that our algorithm consistently outperforms the best representative range-free localization algorithms currently available in the literature in terms of accuracy, even with the presence of non-uniform node distribution or radiation irregularities.

II. NETWORK MODEL

Fig. 1 illustrates the network model of N WSN nodes uniformly deployed in a 2-D square area S in the presence of a rectangle obstacle which makes the network topology C -shaped. All nodes are assumed to have the same transmission capability (i.e., range) denoted by R . Each node is able to directly communicate with any other node located in the disc having that node as a center and R as a radius, while it communicates in a multi-hop fashion with the nodes located outside. Due to the high cost of the global positioning system (GPS) technology, only a few nodes commonly known as anchors are equipped with it and, hence, are aware of their positions. The other nodes, called hereafter position-unaware or regular nodes for the sake of simplicity, are oblivious to this information. As shown in Fig. 1, the anchor nodes are marked with red triangles and the regular ones are marked with black circles. Let N_a and $N_u = N - N_a$ denote the number of anchors and regular nodes, respectively. Without loss of generality, let (x_i, y_i) , $i = 1, \dots, N_a$ be the coordinates of the anchor nodes and (x_i, y_i) , $i = N_a + 1, \dots, N$ those of the regular ones.

Work supported by the CRD, DG, and CREATE PERSWADE www.createperswade.ca Programs of NSERC and a Discovery Accelerator Supplement Award from NSERC.

III. RELATED WORKS AND MOTIVATION

In order to localize the i -th regular node (i.e., $(N_a + i)$ -th node), the distances between it and at least 3 anchors are usually required. The k -th anchor should then broadcast its coordinates (x_k, y_k) through the network. If the i -th regular node is located in the coverage area of this anchor (i.e., the disc $D(k, R)$ having the k -th anchor as center and R as radius), it receives the coordinates in $n_k = 1$ hop. Otherwise, it receives them after $n_k > 1$ hops. So far, in most previous algorithms, the i -th regular node estimates its distance to the k -th anchor $d_{k-(N_a+i)}$ using only the information n_k as

$$\hat{d}_{k-(N_a+i)} = n_k \bar{h}_s \quad (1)$$

where \bar{h}_s is a predefined average hop size. Note that this distance estimation approach relies on the fact that in highly dense WSNs,

$$d_{k-(N_a+i)} \approx \sum_{l=1}^{n_k} h_l, \quad (2)$$

holds. In (2), h_l is the l -th hop's distance. \bar{h}_s is usually derived either analytically (i.e., $\bar{h}_s = E\{h_l\}$) as with LAEP [13] or heuristically as with DV-Hop [6] by computing the mean hop size of all the shortest paths between anchors as follows

$$\bar{h}_s = \frac{1}{N_a(N_a - 1)} \sum_{k=1}^{N_a} \sum_{j=1}^{N_a} \frac{d_{k-j}}{n_{k,j}} \quad (3)$$

where $n_{k,j}$ is the number of hops between the k -th and j -th anchors. Although heuristical and analytical algorithms are proven to be sufficiently accurate in isotropic WSNs (i.e., where obstacles do not exist), their accuracies substantially deteriorate in anisotropic WSNs (AWSN)s. Indeed, in such type of networks, it is very likely that the shortest paths between one regular node and some anchors are not straight lines due to the presence of an obstacle, as can be observed from Fig. 1. This unfortunately causes an overestimation of the distances between the regular node and these anchors, when mapping the number of hops into distance, thereby hindering localization accuracy. In the example of Fig. 1, the regular node 1 communicates with the anchor node A_1 through $n_1 = 6$ hops. Its distance estimate to this anchor $\hat{d}_{k-(N_a+1)}$ is derived using (1). As can be seen from Fig. 1, if the blue obstacle does not exist, n_1 would be much less than 6 and, hence, the distance from i to A_1 is overestimated. Thus, using $\hat{d}_{k-(N_a+i)}$ when performing multilateration will undoubtedly result in an imprecise localization. An interesting approach to circumvent this issue is to properly select the anchors so that overestimation stemming from situations similar to the one illustrated in Fig. 1 is avoided or minimized. Based on this reliable anchor selection, several localization algorithms for AWSNs have been so far proposed such as pattern-driven in [14] and RAL in [15]. Despite their valuables to the advancement of knowledge and know-how in this key topic, we will later see that they still leave room for significant additional accuracy improvements in AWSNs.

In the following, we develop a novel localization algorithm based on new reliable anchor selection strategy and prove that it outperforms all the aforementioned algorithms.

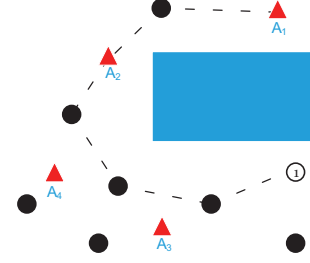


Fig. 1. Network model.

IV. PROPOSED LOCALIZATION ALGORITHM

As a first step of any anchor-based localization algorithm, the k -th anchor broadcasts through the network a message containing (x_k, y_k, n) where n is the hop-count value initialized to one. When a node receives this message, it stores the k -th anchor position as well as the received hop-count $n_k = n$ in its database, adds one to the hop-count value and broadcasts the resulting message. Once this message is received by another node, its database information is checked. If the k -th anchor information exists and the received hop-count value n is smaller than the stored one n_k , the node updates n_k to n , increases it by 1, then broadcasts the resulting message. If n_k is smaller than n , the node discards the received message. However, when the node is oblivious to the k -th anchor position, it adds this information to its database and forwards the received message after increasing n by 1. This mechanism will continue until all nodes become aware of all anchors' positions and their corresponding minimum hop counts. In order to avoid the situation illustrated in Fig. 1, we propose a reliable anchor selection phase in the second step of our algorithm. In the next section, we introduce a new selection strategy where the k -th anchor properly selects a set of reliable anchors among all of those in the network denoted by s_k . The k -th anchor then broadcasts s_k over the network. Upon reception of all (x_k, y_k, n_k, s_k) , $k = 1, \dots, N_a$, each regular node estimates its distance only to its nearest anchor (i.e., $k_0 = \arg \min_k n_k$) and to the reliable anchors in the set s_{k_0} . The regular nodes finally compute their own positions exploiting their available distances' estimates by performing multilateration [16].

In what follows, we develop our proposed reliable anchor selection strategy as well as our distance estimation technique.

V. RELIABLE ANCHOR SELECTION STRATEGY

After receiving all anchors' information, the k -th anchor becomes aware of its own position as well as those of all other anchors in the network and, hence, is able to compute all true distances separating it from the latter. On the other hand, this anchor could also compute the estimate of the distance to any other anchor j and the corresponding estimation error e_{k-j} stemming from the use of (1). Nevertheless, due to the anisotropic topology of the WSN considered here, errors could be too large if we fall in a situation such as in Fig. 1. Consequently, a threshold on e_{k-j} is required to guarantee some reliability of the j -th anchor with respect to the k -th anchor. If the topology of the WSN were isotropic, the estimation error of the distance between these anchors would be

$$T_1 = \hat{d}_{k-j} - d_{k-j} = \lceil \frac{d_{k-j}}{\bar{h}_s} \rceil \bar{h}_s - d_{k-j}, \quad (4)$$

where the second line is due to the fact that \hat{d}_{k-j} is obtained using (1). In (4), $\lceil x \rceil$ refers to the ceiling function. Thus, a distance estimation error higher than T_1 occurs only if the shortest path between the k -th and the j -th anchors is curved due to the presence of obstacles between the two nodes. In such a case, the number of hops between the latter is much larger than d_{k-j}/\bar{h}_s and, hence, we should have $e_{k-j} \gg T_1$. Therefore, we chose T_1 as a threshold below/above which an anchor is deemed reliable or not, respectively. Finally, in order to ensure an accurate distance estimation, each regular node will estimate its distance only to the nearest anchor and to those rated reliable by the latter.

Algorithm 1 Localization algorithm for anchor nodes

```

% k refers to the k-th anchor node %
s_k = {}
for j=1 to N_a and j ≠ k do
    d̂_{k-j} = n_k × h̄_s
    e_{k-j} = d̂_{k-j} - d_{k-j}
    if e_{k-j} ≤ T_1 then
        s_k = s_k ∪ {j}
    end if
end for
Broadcast the set s_k of reliable anchors

```

Algorithm 2 Localization algorithm for regular nodes

```

% i refers to the i-th regular node %
% s_{k_i} is the set of the reliable anchors at the nearest anchor
node from the i-th regular node %
% s_i is the new set of reliable anchors at the i-th regular
node %
s_i = {}
c = 0
for k ∈ s_{k_i} do
    if h_{i-k} ≤ T_2 then
        s_i = s_i ∪ {k}
        c = c + 1
    end if
end for
for j = 1 → c do
    d̂_{j_i} = n_{j_i} × h̄_s
end for
% j_i denotes the j-th reliable anchor node index in the set
s_i %
% x̂_i, and ŷ_i can be estimated using multilateration. %

```

However, some anchors deemed reliable by the nearest anchor could be found unreliable by the regular node, since the shortest path from the latter to these anchors may be curved as shown in Fig. 1. To circumvent this issue, we implement a finer selection at the regular node that discards each anchor having a number of hops larger than $T_2 = \lceil \sqrt{2S}/R \rceil$. Note that T_2 is the maximum number of hops that may occur if the shortest path is not curved. Processing steps at the anchors and regular nodes are summarized by localization algorithms 1 and 2 listed in Algorithms 1 and 2, respectively.

VI. DISTANCE ESTIMATION TECHNIQUE

We propose in this work to estimate each regular-anchor distance using (1). To this end, one should accurately derive

the average hop size \bar{h}_s between any two consecutive nodes on the shortest path between any regular and anchor nodes. Let us consider a two-hop scenario where the k -th node communicates with the i -th node through an intermediate node j . In what follows, we denote by Z and X the random variables that represent the distances d_{k-j} and d_{k-i} , respectively. In order to derive $\bar{h}_s = E\{Z\}$, we start by deriving the conditional cumulative distribution function (CDF) $F_{Z|X}(z)$ of Z with respect to X .

A. Two-dimensional (2-D) case

As can be shown from Fig. 2(a), $Z \leq z$ is guaranteed only if there are no nodes in the area $B_z = F - A_z$ where $F = D(k, R) \cap D(i, R)$, $A_z = F \cap D(k, z)$ and $D(\cdot, \star)$ is the disc having the \cdot -th node as a center and \star as a radius. It is noteworthy that F is nothing but the forwarding zone area where any potential intermediate node must exist. $F_Z(z)$ can be then defined as

$$F_{Z|X}(z) = P(Z \leq z|X) = P(E_0), \quad (5)$$

where $P(E_0)$ is the probability that the event $E_0 = \{\text{no nodes in the area } B_z\}$ occurs.

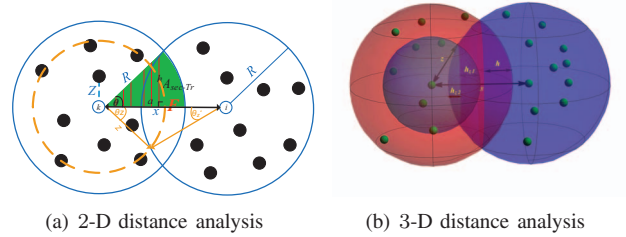


Fig. 2. Distance analysis.

Since the nodes are uniformly deployed in S , the probability of having K nodes in B_z follows a Binomial distribution $\text{Bin}(N, p)$ where $p = \frac{B_z}{S}$. For relatively large N and small p , it can be readily shown that $\text{Bin}(N, p)$ can be accurately approximated by a Poisson distribution $\text{Pois}(\lambda B_z)$ where $\lambda = N/S$ is the average nodes density in the network. Consequently, for a large number of nodes N and small p , we have

$$F_{Z|X}(z) = e^{-\lambda B_z}. \quad (6)$$

As can be seen from Fig. 2(a), $F = 4A_{\text{Sec-Tr}}$ where $A_{\text{Sec-Tr}}$ is the green sector area minus the dashed triangle area. Please note that this equality holds only when the two circles have the same radius R (i.e., the k -th and j -th nodes have the same transmission capability). F is then given by

$$F = 2(R^2\theta - a \times h) = 2R^2 \left(\theta - \frac{\sin(2\theta)}{2} \right). \quad (7)$$

Following the same approach as above, A_z can be obtained as

$$A_z = z^2 \left(\theta_z - \frac{\sin(2\theta_z)}{2} \right) + R^2 \left(\theta'_z - \frac{\sin(2\theta'_z)}{2} \right). \quad (8)$$

Furthermore, using some geometrical properties, we easily show that $\theta_z = \sqrt{\frac{z+R(1-2\cos(\theta))}{2R(1-\cos(\theta))}}\theta$, and $\theta'_z = \sqrt{\frac{R-z}{2R(1-\cos(\theta))}}\theta$.

Substituting θ_z and θ'_z in (8) and using (7), we have

$$B_z = R^2 \left(2\theta - \sin(2\theta) - \theta'_z + \frac{\sin(2\theta'_z)}{2} \right) - z^2 \left(\theta_z - \frac{\sin(2\theta_z)}{2} \right). \quad (9)$$

Substituting (9) in (6) and using the resulting CDF to compute the mean of the random variable Z yields to

$$\bar{h}_s^{2D} = R - \frac{3}{\pi} \int_0^{\frac{\pi}{3}} \int_0^R e^{-\lambda B_z} dz d\theta. \quad (10)$$

Note in (10) that we use the fact that $\theta \in [0, \pi/3]$ since $\theta = \arccos(x/2R)$ where $x \in]R, 2R]$. It follows from (10) that \bar{h}_s^{2D} increases with the nodes density λ . This is expected since it is very likely that the per-hop distance increases when the number of nodes located inside F increases if, of course, R is fixed. From (10), \bar{h}_s^{2D} is also an increasing function of R .

B. Three-dimensional (3-D) case

Since each node is able to communicate with any other node located at most at R meters from it, its transmission coverage in the 3-D case is spherical. Let us denote by V the forwarding zone defined as $V = S(k, R) \cap S(i, R)$ where $S(\cdot, \star)$ is the sphere having the \cdot -th node as a center and \star as a radius. In 3-D case, the CDF $F_{Z|X}(z)$ is then given by

$$F_{Z|X}(z) = e^{-\lambda_v(V-V_z)}, \quad (11)$$

where $V_z = S(k, z) \cap S(i, R)$, $\lambda_v = N/V_T$, and V_T is the total volume where the WSN is deployed. As can be shown from Fig. 2(b), $V = 2V_c$ where V_c is the volume of the spherical cap with height $h = \frac{2R-x}{2}$. Therefore, V is given by $V = \frac{1}{12}\pi(2R-x)^2(4R+x)$.

As far as V_z is concerned, from Fig. 2(b), it is the sum of the volumes of two spherical caps with heights

$$h_{z1} = \frac{(R-z+x)(R+z-x)}{2x} \quad (12)$$

$$h_{z2} = \frac{(R-x+z)(-R+x+z)}{2x}. \quad (13)$$

V_z is then given by

$$V_z = \frac{\pi(R-x+z)^2((x-z)(x+3z)+2R(x+3z)-3R^2)}{12x}. \quad (14)$$

Substituting V and V_z in (11) and using the resulting CDF, we obtain

$$\bar{h}_s^{3D} = R - \frac{1}{R} \int_R^{2R} \int_0^R e^{-\lambda_v(V-V_z)} dz dx. \quad (15)$$

From (15), \bar{h}_s^{3D} is an increasing function of λ_v and R .

VII. SIMULATIONS RESULTS

In this section, we evaluate by simulations the performance of the proposed algorithm in terms of localization accuracy using Matlab. These simulations are conducted to compare, under the same network settings, the proposed algorithm with some of the best representative localization algorithms currently available in the literature, i.e., DV-Hop [6], RAL [15], and pattern-driven [14]. In all simulations, nodes are uniformly deployed in a 2-D square area $S = 10^4 m^2$. Please note that, for the sake of consistency, we only focus in this section on the 2-D case, but all the provided results also hold for the 3-D case. Besides to the C-shaped network topology in Fig. 1, we consider one other anisotropic topology commonly used in the context of WSN: W-shaped [14]. As an evaluation criterion, we propose to use the

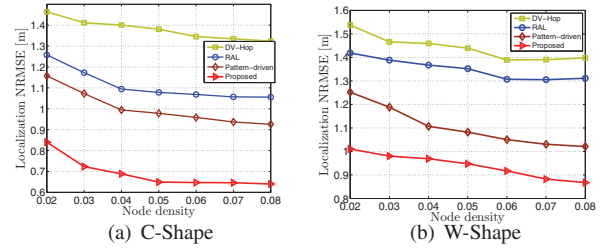


Fig. 3. Localization NRMSE vs. node density with $N_a = 20$ in C- and W-shaped network topologies.

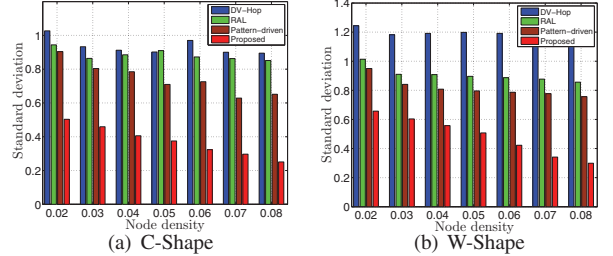


Fig. 4. Localization NRMSE's standard deviation vs. node density with $N_a = 20$ in C- and W-shaped network topologies.

normalized root mean square error (NRMSE) defined as follows

$$e = \frac{\sum_{i=1}^{N_u} \sqrt{(x_i - \hat{x}_i)^2 + (y_i - \hat{y}_i)^2}}{N_u R}. \quad (16)$$

All the following results are obtained by averaging over 100 trials.

Fig. 3 plots the localization NRMSE achieved by DV-Hop, RAL, pattern-driven, and our proposed algorithm versus the node density with a constant number of anchors set to be 20 in C- and W-shaped network topologies. As can be shown from these figures, the proposed algorithm always outperforms its counterparts. Indeed, it is until about 80%, 70% and 60% more accurate than DV-Hop, RAL, and pattern-driven, respectively. Furthermore, our algorithm achieves almost the same performance in the two network topologies while DV-Hop's, RAL's, and driven-pattern's performance, which are already poor in the C-shaped topology, severely deteriorate in the W-shaped topology.

Fig. 4 shows the NRMSEs' standard deviations achieved by all localization algorithms for different node densities in the C- and W-shaped network topologies. As can be seen from these figures, the NRMSEs' standard deviations achieved by DV-Hop, RAL, and driven-pattern slightly decrease when the node density increases while the one achieved by the proposed algorithm substantially decreases. This means that implementing our algorithm in any network topology guarantees an accurate localization for any given realization. This result is very interesting in terms of implementation strategy, since it proves that the result in Fig. 3 becomes more and more meaningful as λ grows large.

Fig. 5 illustrates the localization NRMSE's CDF achieved by DV-Hop, RAL, pattern-driven, and our proposed algorithm with $N = 200$ and $N_a = 20$ in the C- and W-shaped network topologies. Using the proposed algorithm, until 80% of the regular nodes could estimate their position within twice the transmission range. In contrast, until 38% and 42% of the nodes achieve the same accuracy with RAL and pattern-driven, respectively, and about 0% with DV-Hop. This further proves the efficiency of our

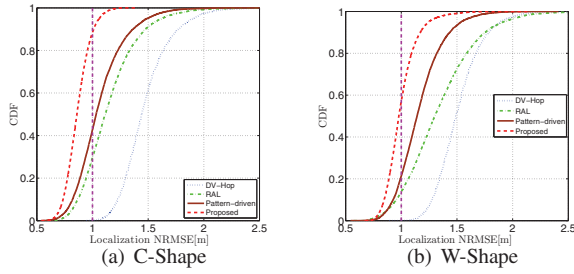


Fig. 5. Localization NRMSE's CDF with $N = 200$ and $N_a = 20$ in C- and W-shaped network topologies.

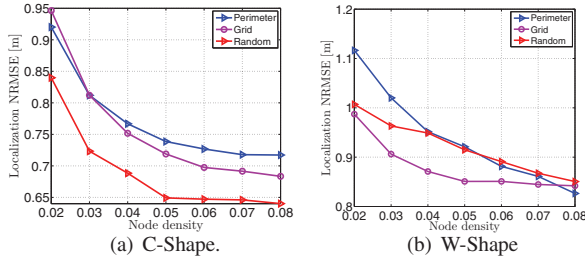


Fig. 6. Proposed algorithm's NRMSE vs. anchors' placements in C- and W-shaped network topologies.

new algorithm.

Fig. 6 plots the localization NRMSEs achieved by the proposed algorithm and its counterparts versus the nodes density with different anchors placement strategies: perimeter, grid and random, respectively. This figure shows that the grid anchors' placement is the most efficient strategy in W-shaped topology while the random anchors' placement is best in the C-shaped topologies. This result is very interesting since it proves that the performance of each strategy is closely related to the network topology. In other words, if the latter is known beforehand, we will be able to select the appropriate strategy when deploying the WSN.

Figs. 7(a) and 7(b) plot the localization NRMSEs achieved by the proposed algorithm and its counterparts versus the nodes density and the degree of range irregularity (DoI), respectively. In Fig. 7(a), a non-uniform nodes' deployment is assumed while, in Fig. 7(b), the transmission range is no longer assumed circular. A range irregularity model similar to that in [17] was implemented instead. From these figures, the localization NRMSEs achieved by all algorithms deteriorate due to both non-uniform nodes' deployment and range irregularity. This is expected since these phenomena are not taken into account when designing the proposed algorithm and its counterparts. However, as could be observed from Figs. 7(a) and 7(b), the proposed algorithm remains more accurate than its counterparts. This further proves the increased robustness of our proposed algorithm to model imperfections.

VIII. CONCLUSION

In this paper, we proposed a novel range-free localization algorithm tailored for anisotropic WSNs. Using the proposed algorithm, each regular node estimates its distances to reliable anchors only. The latter are properly chosen following a new reliable anchor selection strategy that ensures an accurate distance estimation thereby making our localization algorithm more precise. New average hop sizes' expressions were also developed

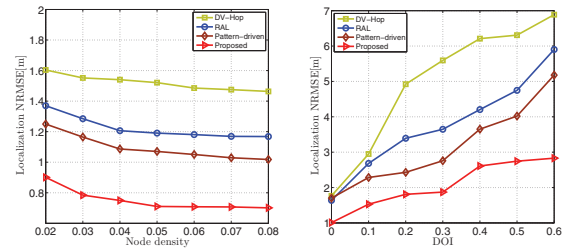


Fig. 7. Localization NRMSE vs. DOI and non-uniform nodes' deployment with $N_a = 20$ and in C-shaped network topology.

in this paper for both 2-D and 3-D scenarios. Simulations showed that our algorithm consistently outperforms the best representative range-free localization algorithms currently available in the literature in terms of accuracy, even with the presence of non-uniform node distribution or radiation irregularities.

REFERENCES

- [1] F. Gustafsson and F. Gunnarsson, "Mobile Positioning Using Wireless Networks: Possibilities and Fundamental Limitations Based on Available Wireless Network Measurements," *IEEE Signal Process. Mag.*, vol. 22, no. 4, pp. 41-53, July 2005.
- [2] F. Akyildiz, W. Su, Y. Sankarasubramaniam, and E. Cayirci, "A Survey on Sensor Networks," *IEEE Commun. Mag.*, vol. 40, no. 8, pp. 102-114, August 2002.
- [3] N. Patwari, A. O. Hero III, M. Perkins, N. S. Correal and R. J. O'Dea, "Relative Location Estimation in Wireless Sensor Networks," *IEEE Trans. Signal Process.*, vol. 51, no. 8, pp. 2137-2148, August 2003.
- [4] D. Niculescu and B. Nath, "Ad Hoc Positioning System (APS) Using AOA," *IEEE INFOCOM'2003*, vol. 3, pp. 1734-1743, 2003.
- [5] H. Ren and M. Q.-H. Meng, "Power Adaptive Localization Algorithm for Wireless Sensor Networks Using Particle Filter," *IEEE Trans. Veh. Technol.*, vol. 58, no. 5, pp. 2498-2508, June 2009.
- [6] D. Niculescu and B. Nath, "Ad hoc Positioning System (APS)," *Proc. IEEE GlobeCom'2001*, Nov. 25-29, 2001.
- [7] A. El Assaf, S. Zaidi, S. Affes, and N. Kandil, "Range-Free Localization Algorithm for Heterogeneous Wireless Sensors Networks," *IEEE WCNC'2014*, Istanbul, Turkey, Apr. 6-9, 2014.
- [8] A. EL Assaf, S. Zaidi, S. Affes, and N. Kandil, "Accurate Nodes Localization in Anisotropic Wireless Sensor Networks," *International Journal of Distributed Sensor Networks*, vol. 2015, Article ID 105682, 17 pages, 2015. doi:10.1155/2015/105682
- [9] A. EL Assaf, S. Zaidi, S. Affes, and N. Kandil, "Cost-effective and Accurate Nodes Localization in Heterogeneous Wireless Sensor Networks," *Proc. IEEE ICC'2015*, London, United Kingdom, June. 8-12, 2015.
- [10] A. EL Assaf, S. Zaidi, S. Affes, and N. Kandil, "Range-free localization algorithm for anisotropic wireless sensor networks," *Proc. IEEE VTC'2014-Fall*, Vancouver, Canada, Sep. 14-17, 2014.
- [11] A. EL Assaf, S. Zaidi, S. Affes, and N. Kandil, "Efficient range-free localization algorithm for randomly distributed wireless sensor networks," *Proc. IEEE GLOBECOM'2013*, Atlanta, GA, USA, Dec. 9-13, 2013.
- [12] A. EL Assaf, S. Zaidi, S. Affes, and N. Kandil, "Hop-Count Based Localization Algorithm for Wireless Sensor Networks," *Proc. IEEE MMS'2013 (Invited Paper)*, Saida, Lebanon, September 2-5, 2013.
- [13] Y. Wang, X. Wang, D. Wang, and D. P. Agrawal, "Range-Free Localization Using Expected Hop Progress in Wireless Sensor Networks," *IEEE Trans. Parallel Distrib. Syst.*, vol. 25, no. 10, pp. 1540-1552, October 2009.
- [14] Q. Xiao, B. Xiao, J. Cao, J. Wang, "Multihop Range-Free Localization in Anisotropic Wireless Sensor Networks: A Pattern-Driven Scheme," *IEEE Trans. Mobile Comput.*, vol. 9, no. 11, pp. 1592-1607, November 2010.
- [15] B. Xiao, L. Chen, Q. Xiao, and M. Li, "Reliable Anchor-Based Sensor Localization in Irregular Areas," *IEEE Trans. Mobile Comput.*, vol. 9, no. 1, pp. 60-72, January 2010.
- [16] D. E. Manolakis, "Efficient Solution and Performance Analysis of 3-D Position Estimation by Trilateration," *IEEE Trans. Aerosp. Electron. Syst.*, vol. 32, no. 4, pp. 1239-1248, October 1996.
- [17] S. Biaz, Ji. Yiming, Q. Bing, Wu. Shaoen, "Realistic radio range irregularity model and its impact on localization for wireless sensor networks," *IEEE WiCOM'2005*, Wuhan, China, Sept. 23-26 2005.